Polym. Bull. (2009) 62:801–811
DOI 10.1007/s00289-009-0060-0

ORIGINAL PAPER

# Microstructure and properties of silane monomer-modified styrene-acrylate nanocoatings

**Tao Wan · Chuan Wu · XiaoLing Ma · Lan Wang · Jie Yao · Kuai Lu**

Received: 7 October 2008 / Revised: 15 December 2008 / Accepted: 24 February 2009 /
Published online: 14 March 2009


**Abstract** Microstructure and properties of silane monomer-modified styrene-acrylate nanocoatings by photopolymerization were investigated using TEM, TGA, FTIR and UV–Vis measurements. The transmittances of the microemulsions and final nanolatexes as well as the acid and base resistances of the final nanolatexes decrease and acid, base and water resistances of the nanocoatings increase with increase in the monomer to surfactant mass ratio and $\gamma$-methacryloxypropyltrimethoxysilane (KH570) content. The polymer particles are nearly spherical and are very uniform with the number average particle size of 25.5 nm and Dw/Dn of 1.11. FTIR spectrum indicates the possible structure of the organosilicone modified styrene-acrylate copolymer.

**Keywords** Nanolatexes · Microemulsion · Photopolymerization · Coating

## Introduction

Polymerization in oil in water microemulsions can prepare the ultrafine latex particles in the size range 10–100 nm with narrow size distribution. The polymerized nanolatexes are expected to be environmentally friendly and have immense potential in industrial and pharmaceutical applications. Therefore,

T. Wan (✉) · X. Ma · L. Wang · J. Yao · K. Lu
College of Materials and Chemistry & Chemical Engineering, Chengdu University of Technology, 610059 Chengdu, China
e-mail: wantaos@sohu.com

T. Wan · C. Wu
Key Laboratory of Organosilicon Chemistry and Material Technology of Ministry of Education, Hangzhou Normal University, 310012 Hangzhou, China

microemulsion polymerization has attracted great interest and become an increasingly growing field of research in polymer synthesis [1–5].

Photopolymerization has rapidly expanded as an industrial technology because of its main advantages: the process is energy-efficient and generally economical. It has found extensive applications in producing photoactive polymer systems used in coatings, paints, inks, composites, and restorative dental formulations. Compared with thermo-induced polymerization, UV-induced polymerization is more rapid and can be carried out at lower temperature, such as room temperature [6–8].

Photopolymerizations in microemulsion systems are particularly attractive because of their good optical transparencies, high polymerization rates and low reaction temperature. Therefore, the photo-induced microemulsion polymerization is found to be very efficient for the preparation of very fine nanolatexes at room temperature. By far, the monomers most extensively studied by microemulsion polymerization are acrylate [9–13] and styrene [14–16]. For example, Jain [9] studied the butyl acrylate microemulsion photopolymerization using a two-component initiator system comprised of Rose Bengal (RB) and methyldiethanolamine (MDEA) and found these compounds underwent photo-induced electron transfer upon absorption of 550 nm light to produce amine radicals active in free radical polymerization. Capek et al. [11] obtained stable and bluish-translucent microlatexes containing spherical poly (butyl acrylate) particles with diameters ranging from 30 to 50 nm by photopolymerizations of transparent o/w microemulsions of SDS/water/BA. David [12] investigated MMA and BA photopolymerization in oil-in-water microemulsions with SDS as surfactant and poly (*N*-acetylethylenimine) (PNAEI) macromer as cosurfactant and a comonomer. The average diameters of latex particles were in the range of 17–200 nm. Turro et al. [14] reported photoinitiated microemulsion polymerization of styrene with dibenzyl ketone (DBK) as an initiator and UV light with wavelength 313 nm as an initiating source. The system remains transparent during the whole polymerization process and the particle sizes of the produced latexes are in the range of 30–60 nm with the polydispersity indexes of 1.05–1.08. Wang [15] has synthesized the first water-soluble perester ([4-(4-tert-butyldioxycarbonylbenzoyl)-benzyl] trimethylammonium chloride) that can serve as an amphiphilic initiator (PAI). Small nanoparticles with diameter approximately 29 nm were formed by the PAI initiated photopolymerization. However under similar conditions the PAI initiated polymerization (at 70 °C) formed the latex particles with diameter approximately 40 nm. Wan [16] prepared a relatively concentrated silane monomer-modified styrene-acrylate microemulsion coating with high monomer to surfactant ratio of 7.5:1 by microemulsion photopolymerization, using benzophenone (BP) and Michler's ketone (MK) as mixed photoinitiators.

However the microemulsion copolymerization of styrene and butyl acrylate in the presence of silane coupling agent, such as $\gamma$-methacryloxypropyltrimethoxysilane (KH570), has been scarcely studied, especially by photopolymerization using 2-hydroxy-2-methylpropiophenone as photoinitiator. This paper presents an attempt to investigate the microstructure and properties of nanocoatings formed by photopolymerization using TEM, TGA, FTIR and UV–Vis measurements. It is an

easy, rapid, inexpensive and environmentally friendly method to produce transparent and stable nanolatexes without flocculation and aggregation.

## Experimental

### Materials

Sodium dodecyl sulfate (SDS) and 1-pentanol were analytical grade; butyl acrylate(BA), styrene(ST) were received from the Chengdu Kelong Chemical Co and washed by 20% NaOH solution three times before use. Silane coupling agent $\gamma$-methacryloxypropyltrimethoxysilane (KH570) from Nanjing Shuguang Organosilicone Co; 2-hydroxy-2-methylpropiophenone from Aldrich and was used without further purification; Distilled water was used in all experiments.

### Microemulsion photopolymerization

A 125 ml glass reactor with magnetic stirring was employed to form 100 ml of microemulsion with a composition by weight percent of 4/2/10/1/100 SDS/1-pentanol/(BA + ST)/KH570/$H_2O$ and ST/BA ratio of 70/30 by weight, where SDS was used as surfactant and 1-pentanol as cosurfactant. After stirring for about 30 min to allow the microemulsion to come to a thermodynamic equilibrium, about 0.3 g photoinitiator 2-hydroxy-2- methylpropiophenone were added into the above transparent microemulsions. Finally the microemulsions were poured into the precleaned glass vessel. Microemulsion photopolymerization was achieved by irradiating the samples with a 500 W high pressure mercury lamp for about 30–45 min UV irradiation.

### Acid and alkali resistance of the final nanolatexes

10% HCl and 10% NaOH solution are added dropwise into the final nanolatexes and visual inspection of coagulum and flocculation are evaluated for the acid, base resistance of the nanolatexes.

### Acid and alkali resistance of the microemulsion coatings

Microemulsion coatings were cast onto glass at ambient temperature. After drying at room temperature, the coated glass was immersed into 10% HCl and 10% NaOH solution, respectively, and visual inspection of blister and cracks were evaluated for the acid and alkali resistance of the microemulsion coatings. All the tests were conducted at ambient temperature.

### Swelling test of the microemulsion coatings

The microemulsion coatings were cut into small pieces. They were then swelled in water at 30 °C until they reached equilibrium, and their gains in weight were

recorded. Duplicate readings were taken for each sample. The dried weight of each polymer sample was obtained by drying it in a vacuum oven at room temperature until a constant weight was attained. The equilibrium water content (EWC) of the microemulsion coatings is defined as

$$\mathrm{EWC} = (W_s - W_0)/W_s \times 100 \quad (1)$$

where $W_0$ and $W_s$ represent the weight of the dried and swollen coatings, respectively.

### Characterizations

UV–Vis absorption spectra were recorded on a Thermo Spectronic Genesys TM 10 series spectrophotometer with a quart cuvette possessing an optical path length of 1 cm. The microemulsion was precipitated by ethanol and the surfactants were removed by water and methanol to obtain the copolymers for FTIR characterization. Infrared spectrum of copolymers was taken with a 510 Nicolet FTIR spectrometer. The transmission electron microscopy was performed on H-600 type instrument. TGA was measured on a Dupont 2100 instrument. The temperature program was 10.0 K/min from 20 to 500 °C under $N_2$ atmosphere.

## Results and discussions

### Effects of monomer to surfactant mass ratio on the UV–Vis spectra of the microemulsions and final nanolatexes

Figure 1 indicates the effects of monomer to surfactant mass ratio on the absorbency and transmittance of the microemulsions. As shown in Fig. 1, with increase of monomer to surfactant mass ratio, the absorbencies increase in the range of 300–400 nm and the transmittances decrease in the range of 400–500 nm, although both of them show good transparencies due to the high transmittance in the visible light

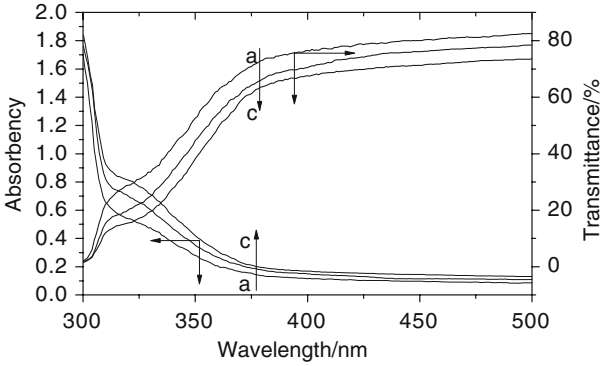


**Fig. 1** Effects of monomer to surfactant mass ratio on the absorbency and transmittance of the microemulsions, monomer to surfactant mass ratio (**a**) 8/10 (**b**) 10/10 and (**c**) 12/10 with 6% KH570

region. Above all, microemulsions with different monomer to surfactant mass ratio are suitable for photochemical reactions because of their transparent properties in the visible region and high absorbency in the UV light region due to the 1.5% photoinitiator in the microemulsions.

Effects of monomer to surfactant mass ratio on the transmittance of the final nanolatexes are shown in Fig. 2. Transmittances of the nanolatexes decrease with increase in monomer to surfactant mass ratio. As more monomer is added, the sizes of monomer-solubilized micelles enlarge and the interdroplet attractive interactions increase. Therefore latex sizes increase with an increase in monomer to surfactant mass ratio, and the transmittances of the nanolatexes turn from 73 to 63% at 600 nm with increase in monomer to surfactant mass ratio from 8/10 to 12/10.

## Effects of KH570 content on the UV–Vis spectra of the microemulsions and final nanolatexes

Figure 3 plots the absorbency and transmittance of the microemulsions as a function of the KH570 content. As shown in Fig. 3, with an increase of KH570 content from 6 to 10%, based on the monomer weight, the absorbencies and transmittances of the

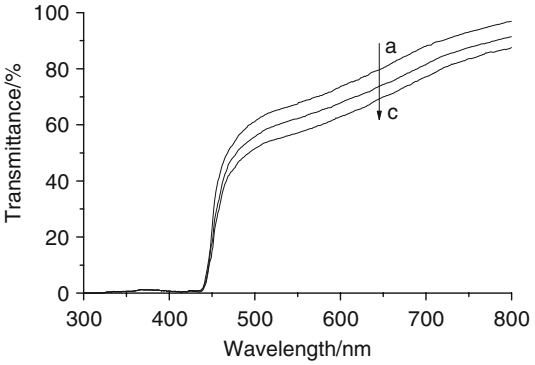


**Fig. 2** Effects of monomer to surfactant mass ratio on the transmittance of the final nanolatexes, monomer to surfactant mass ratio (**a**) 8/10 (**b**) 10/10 and (**c**) 12/10 with 6% KH570

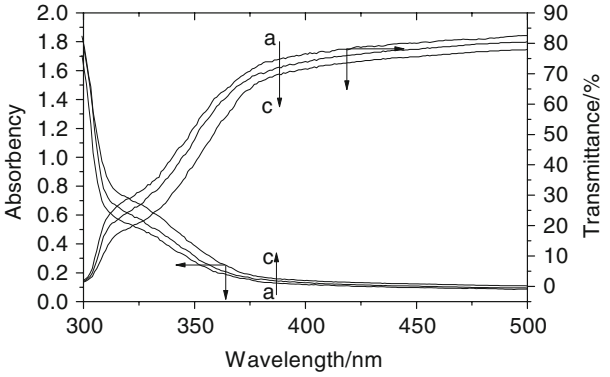


**Fig. 3** Effects of KH570 content on the absorbency and transmittance of the microemulsions, KH570 content (**a**) 6% (**b**) 8% and (**c**) 10% with 8% monomer and 10% SDS

microemulsions change slightly. Therefore it is possible to increase the KH570 content without the large expense of transparency of the microemulsions.

Effects of KH570 content on the transmittance of the final nanolatexes are shown in Fig. 4. Transmittances of the nanolatexes decrease with increase in KH570 content. During photopolymerization, KH570 molecule will hydrolyze partially to form SiOH groups, and these groups residing at the polymer particle surface will condensate each other gradually and there exist some Si–O–Si linkages between the polymer particles which link the particles together and enlarge the polymer particle size. Therefore, the transmittances of the final nanolatxes decrease with KH570 content.

As can be seen from Figs. 1, 2, 3 and 4, although the transmittance of the final nanolatexes are smaller than those of the microemulsions, the final nanolatexes still exhibited good optical transparencies in the visible range (500–760 nm), suggesting the lack of macroscopic organic–inorganic phase separation, so the polymer particles may be dispersed in the water phase in a nanoscale.

## TEM of the microemulsions formed by photopolymerization

The number average diameter ($D_n$) and the weight average diameter ($D_w$) can be calculated from the following equations.

$$D_n = \sum N_i D_i \Big/ \sum N_i \tag{2}$$

$$D_w = \sum N_i D_i^4 \Big/ \sum N_i * \Delta_i \tag{3}$$

The particle size distribution is expressed by the ratio $D_w/D_n$. The $D_w/D_n$ values ranging from 1.0 to 1.1 are regarded as monodisperse distributions of particle sizes, and those ranging from 1.1 to 1.2, as nearly monodisperse distributions.

TEM and particle size and size distribution of the produced latexes are shown in Fig. 5. As indicated by Fig. 5, the polymer particles are nearly spherical and are very uniform with the number average particle size of 25.5 nm and $D_w/D_n$ of 1.11.

Combining the results of Figs. 1, 2, 3, 4 and 5, very important information is obtained, namely that the nanosized polymer particles can be obtained conveniently and rapidly by the microemulsion photopolymerization using 2-hydroxy-2-methylpropiophenone as photoinitiator. This result is very important

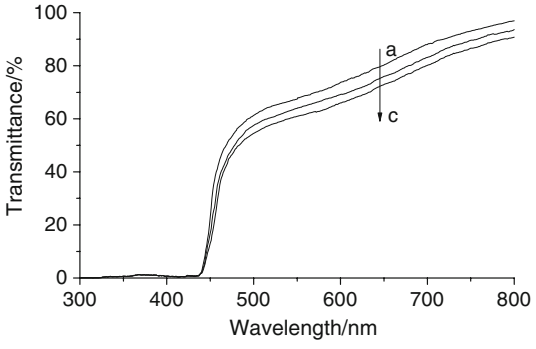


**Fig. 4** Effects of KH570 content on the transmittance of the final nanolatexes, KH570 content (**a**) 6% (**b**) 8% and (**c**) 10% with 8% monomer and 10% SDS

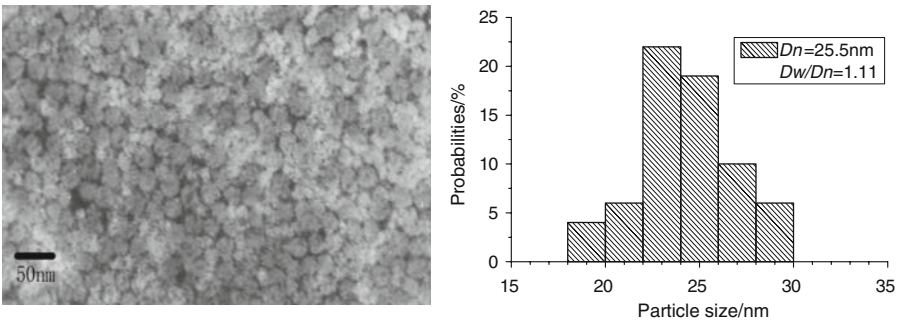


**Fig. 5** TEM (*left*) and particle size and size distribution (*right*) of the silane monomer-modified styrene-acrylate microemulsions, monomer = 8%, SDS = 10%, KH570 = 6%, photoinitiator = 1.5%

and practical, and useful for industrialization of the microemulsion polymerization technique.

## Thermal stability of the nanocoatings

To further corroborate the possible interactions between the polymeric particles by way of condensations of Si–OH residing at the surfaces of the particles, TGA measurements of the nanocoatings were carried out and the results are shown in Fig. 6. From the differential curves of TGA (DTGA) the temperature at which there is a maximum mass loss rate ($T_{max}$), as well as the decomposition onset temperature ($T_{onset}$), is considered a parameter for the estimation of the thermal stability. As shown in Fig. 6, Sample (a) (KH570 = 6%) exhibits a gradual mass loss starting from 50 to 157 °C,which can be mainly attributed to the removal of absorbed water and surfactant in the microemulsion coatings, and shows the $T_{onset}$ of 338 °C and $T_{max}$ of 379 °C with DTGAmax of 5.2%/min. Compared with Sample (a), Sample (b)(KH570 = 10%) shows an enhanced thermal stability with $T_{onset}$ of 347 °C and $T_{max}$ of 387 °C with $DTGA_{max}$ of 6.9%/min.

More KH570 will favor more SiOH and thus more Si–O–Si bonds which will combine the polymer particles together and increase the crosslinking density.

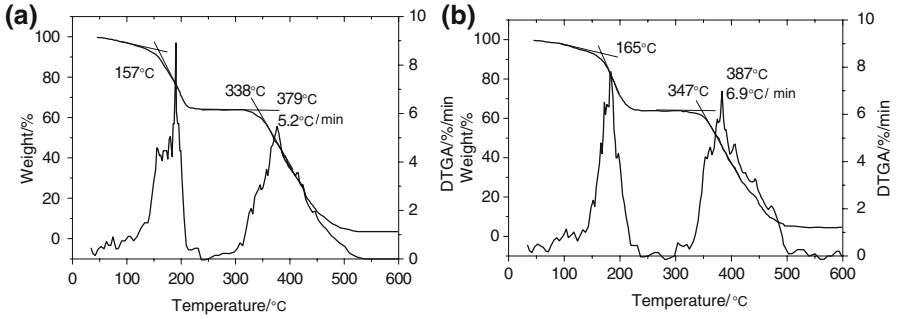


**Fig. 6** Thermal stability of the nanocoatings, KH570 content = 6% (**a**) and 10% (**b**)

Therefore the polymeric chain segment mobility is restrained and the higher amount of Si–O–Si linkages between the polymer particles, the higher temperatures to decompose the organic chains.

## FTIR spectrum of the silane monomer-modified styrene-acrylate copolymers

The FTIR spectrum of the organosilicone modified styrene-acrylate copolymers is shown in Fig. 7. There exist major absorption bands associated with acrylate molecules, such as the asymmetrical stretching of $CH_3$ at 2,968 $cm^{-1}$, and the asymmetrical and symmetrical stretching of–$CH_2$– at 2,918, 2,854 $cm^{-1}$ respectively; The characteristic band at 1,732 $cm^{-1}$ can be attributed to the C=O stretching, and the C–O stretching vibration is designated at 1,120 $cm^{-1}$;1,598 and 1,499 $cm^{-1}$ can be assigned to the benzene stretching vibration. The absorption band of 1,065 $cm^{-1}$ is corresponding to Si–O–Si stretching [17–19]. In the high wave number spectral range 3,450 $cm^{-1}$ is assigned to fundamental stretching vibration of different O H hydroxyl groups. In the low wave number spectral range a not very sharp peak at 950 $cm^{-1}$ is assigned to SiOH species produced from incomplete condensation [19, 20]. All of the above data indicate the possible structure of the organosilicone modified styrene-acrylate copolymers.

## Acid and base resistance of the nanolatexes

The acid and base-resistance of the nanolatexes with different compositions are shown in Table 1. It is noteworthy that the nanolatexes gradually turn from transparent to milk white but still keep stable after more than 15 ml 10% HCl solution is added dropwise into the nanolatexes. However, some coagulations and flocculations occur if more than several milliliters of 10% NaOH solution are added dropwise into the nanolatexes. Besides, the base resistances of the nanolatexes increase with decrease in the mass ratio of monomer to surfactant and KH570 content.

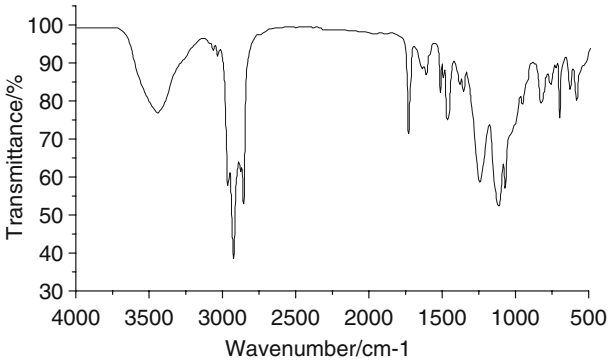


**Fig. 7** FTIR spectrum of the silane monomer-modified styrene-acrylate copolymers

**Table 1** Acid and base-resistance of the final nanolatexes

| Samples | 10% HCl | 10% NaOH |
|---|---|---|
| A | No coagulum (>15 ml) | Coagulum (2.5 ml) |
| B | No coagulum (>15 ml) | Coagulum (0.66 ml) |
| C | No coagulum (>15 ml) | Coagulum (1.9 ml) |

Sample A: monomer/KH570/SDS/1-pentanol/$H_2O$ = 8/0.48/10/5/100
Sample B: monomer/KH570/SDS/1-pentanol/$H_2O$ = 8/0.8/10/5/100
Sample C: monomer/KH570/SDS/1-pentanol/$H_2O$ = 10/0.6/10/5/100

**Table 2** Acid and base resistance of the microemulsion coatings with different compositions

| Samples | Acid resistance | Base-resistance | EWC/% |
|---|---|---|---|
| Sample A | 60 min blister | 80 min blister | 15 |
| Sample B | 150 min blister | 180 min blister | 8.3 |
| Sample C | 70 min blister | 90 min blister | 12.6 |

Sample A: monomer/KH570/SDS/1-pentanol/$H_2O$ = 8/0.48/10/5/100
Sample B: monomer/KH570/SDS/1-pentanol/$H_2O$ = 8/0.8/10/5/100
Sample C: monomer/KH570/SDS/1-pentanol/$H_2O$ = 10/0.6/10/5/100

As more monomer and less surfactant are added, the particle surface coverage ratio of surfactant decreases and interdroplet attractive interactions increase, leading to fusion and mass exchange and resulting in an decrease of base resistances. With increase in KH570 content, more and more Si–O–Si linkages will formed by condensation and they bind the particles together and therefore decrease the chemical resistance of the final nanolatexes.

Under base treatment, it is easy for KH570 molecule to form a network of uniform particles by condensation. So base–treatment accelerates the polcondensation of silanol groups in the nanolatexes [21] to form the Si–O–Si bonds which link the interparticles together and result in coagulation and flocculation. On the other hand, under acid treatment the hydrolysis rate is higher than that of condensation, and acid catalysis promotes the development of more linear or randomly branched chains [22]. Therefore there exist little Si–O–Si linkages between the particles and no coagulation and flocculation occur even if excess amount of HCl solution is added into the nanolatexes.

Acid, base and water resistance of the nanocoatings with different compositions

Table 2 indicates the acid and base resistance of the nanocoatings with different compositions. As shown in Table 2, acid, base and water resistance of the nanocoatings decreased with monomer to surfactant mass ratio decreasing from 10/10 to 8/10. Because of the amphiphilic structure of the surfactant SDS, more SDS in the nanocoatings will do harm to the acid, base and water resistance of the

nanocoatings. However, with increase of KH570 content, the acid, base and water of the nanocoatings upgrade. As indicated by FTIR spectrum, the formation of Si–O–Si linkage will increase the cross-linking degree [23, 24] and thereby increase the acid and base resistance of the silane monomer-modified styrene-acrylate nanocoatings.

## Conclusions

Transparent organosilicone modified styrene-acrylate nanocoatings were prepared by microemulsion photopolymerization within 30 min UV irradiation at room temperature. The transmittances of the microemulsions and final nanolatexes as well as the acid and base resistances of the final nanolatexes decrease and acid, base and water resistances of the nanocoatings increase with increase in the monomer to surfactant mass ratio and KH570 content. The final polymer latexes are transparent with high transmittance in the visible range. The polymer particles are nearly spherical and are very uniform with the number average particle size of 25.5 nm and narrow size distribution. FTIR spectrum indicates the possible structure of the organosilicone modified styrene-acrylate copolymer, and confirms the hydrolysis and condensation resulting in siloxane bonds between polymer particles.

**Acknowledgments** The authors gratefully acknowledge the financial support of Laboratory of Organosilicon Chemistry and Material Technology of Ministry of Education (No. yjg200605).

## References

1. He GW, Pan QM, Rempel GL (2003) Synthesis of poly(methyl methacrylate) nanosize particles by differential microemulsion polymerization. Macromol Rapid Commun 24:585–588
2. Chen J, Zhang ZC (2007) Radiation-induced polymerization of methyl methacrylate in microemulsion with high monomer content. Eur Polym J 43(4):1188–1194
3. Lim TH, Tham MP, Liu ZL, Hong L, Guo B (2007) Nano-structured proton exchange membranes molded by polymerizing bi-continuous microemulsion. J Membr Sci 290(1/2):146–152
4. Katime I, Arellanoa J, Schulz P (2006) Poly(*n*-hexyl methacrylate) polymerization in three-component microemulsion stabilized by a cationic surfactant. J Colloid Interface Sci 296:490–495
5. Wan T, Wang YC, Feng F (2006) Structure and thermal properties of titanium dioxide-polyacrylates nanocomposites. Polym Bull 56:413–426
6. Wan T, Wang YC, Feng F (2006) Preparation of titanium dioxide/polyacrylate nanocomposites by sol–gel process in reverse micelles and in-situ photopolymerization. J Appl Polym Sci 102:5105–5112
7. Peinado C, Bosch P, Martin V, Corrales T (2006) Photoinitiated polymerization in bicontinuous microemulsions: fluorescence monitoring. J Polym Sci Part A Polym Chem 44:5291–5303
8. Wan T, Feng F, Ran R, Wang YC (2006) Photo-differential scanning calorimetry study on photopolymerization of nanosized titanium dioxide/polyacrylate hybrid materials. Polym Int 55(8):883–890
9. Jain K, Klier J, Scranton AB (2005) Photopolymerization of butyl acrylate-in-water microemulsions: polymer molecular weight and end-groups. Polymer 46:11273–11278
10. Capek I (2000) Photopolymerization of alkyl(meth)acrylates and polyoxyethylene macromonomers in fine emulsions. Eur Polym J 36:255–263
11. Capek I, Fouassier JP (1997) Kinetics of photopolymerization of butyl acrylate in direct micelle. Eur Polym J 33(2):173–181

12. Capek I (1996) Photopolymerization of butyl acrylate microemulsions 1. Post-polymerization. Polym Int 40:41–49
13. David G, Ozer F, Simionescu BC, Zareie H, Piskin E (2002) Microemulsion photopolymerization of methacrylates stabilized with sodium dodecyl sulfate and poly(*N*-acetylethylenimine) macromonomers. Eur Polym J 38:73–78
14. Kuo P, Turro NJ, Tseng C, El-Aasser MS, Vanderhoff JW (1987) Photoinitiated polymerization of styrene in microemulsions. Macromolecules 20(6):1216–1221
15. Wang L, Liu X, Li Y (1998) Synthesis and evaluation of a surface-active photoinitiator for microemulsion polymerization. Macromolecules 31:3446–3453
16. Wan T, Hu ZW, Ma XL, Yao J, Lu K (2008) Synthesis of silane monomer-modified styrene-acrylate microemulsion coatings by photopolymerization. Prog Org Coat 62:219–225
17. Li YS, Wright PB, Puritt R, Tran T (2004) Vibrational spectroscopic studies of vinyltriethoxysilane sol–gel and its coating. Spectrochim Acta Part A 60:2759–2766
18. Bosch P, Monte DF, Mateo JL, Levy D (1996) Photopolymerization of hydroxyethylmethacrylate in the formation of organic-inorganic hybrid sol–gel matrices. J Polym Sci Part A Polym Chem 34:3289–3296
19. Morija Y, Sonoyama M, Nishikawa F, Hino R (1993) Preparation of polymer hybrids of the silica-PVA or silica-PEG system and porous materials made from the hybrid gels. J Ceram Soc Jpn 101:518–521
20. Wung CJ, Pang Y, Prasad PN, Karasz FE (1991) Poly(para-phenylene vinylene) silica composite—a novel sol–gel processed nonlinear optical material for optical wave-guides. Polymer 32:605–608
21. Ying JY, Benziger JB (1992) Structural tailoring of alkoxide silica. J Non-Cryst Solids 147:222–231
22. Yoldas BE (1986) Zirconium oxides formed by hydrolytic condensation of alkoxides and parameters that affect their morphology. J Mat Sci 21:1080–1086
23. Du YJ, Damron M, Tang G, Zheng H, Chu C, Osborne JH (2001) Norganic/organic hybrid coatings for aircraft aluminum alloy substrates. Prog Org Coat 41:226–232
24. Palanivel V, Zhu D, Ooij WJV (2003) Nanoparticle-filled silane films as chromate replacements for aluminum alloys. Prog Org Coat 47:384–392